

Copper coordination polymers constructed from thiazole-5-carboxylic acid: synthesis, crystal structures, and structural transformation

Natthaya Meundaeng^a, Apinpus Rujiwatra^a, Timothy J. Prior^{b,*}

^aDepartment of Chemistry, Faculty of Science, Chiang Mai University, Chiang Mai, 50200, Thailand

^bChemistry, University of Hull, Kingston upon Hull, HU6 7RX, UK

*To whom the correspondence should be addressed.

Chemistry, University of Hull, Kingston upon Hull, HU6 7RX, UK, Tel: +44 (0)1482 466389,

Fax: +44 (0)1482 466410, E-mail: t.prior@hull.ac.uk

ABSTRACT

We have successfully prepared crystals of thiazole-5-carboxylic acid (5-Htza) (**L**) and three new thiazole-5-carboxylate-based Cu^{2+} coordination polymers with different dimensionality, namely, 1D $[\text{Cu}_2(5\text{-tza})_2(1,10\text{-phenanthroline})_2(\text{NO}_3)_2]$ (**1**), 2D $[\text{Cu}(5\text{-tza})_2(\text{MeOH})_2]$ (**2**), and 3D $[\text{Cu}(5\text{-tza})_2]\cdot\text{H}_2\text{O}$ (**3**). These have been characterized by single crystal X-ray diffraction and thermogravimetry. Interestingly, the 2D network structure of **2** can directly transform into the 3D framework of **3** upon removal of methanol molecules at room temperature. **2** can also undergo structural transformation to produce the same 2D network present in the known $[\text{Cu}(5\text{-tza})_2]\cdot 1.5\text{H}_2\text{O}$ upon heat treatment for 2 hours. This 2D network can adsorb water and convert to **3** upon exposure to air.

Keywords: Copper, Heterocycles, Supramolecular chemistry, Coordination polymer, Structural transformation

1. Introduction

Self-assembly of organic, inorganic and metal-organic species as molecular building blocks through intermolecular non-covalent bond interactions such as hydrogen bonds [1,2], π - π stacking and other weak interactions [3], has led to the formation of 1D, 2D and 3D supramolecular frameworks. Notable interest has been focused on the crystal engineering of these supramolecular structures, particularly after the discovery that the resulting materials have many specific practical applications [4–8].

To direct assemblies based on coordination chemistry, many factors have to be considered, including choice of ligands [9,10], counter ions [11–13], metal ions [14,15], solvent [16], temperature [17–19], and *etc.* Even considering these factors, reasoned selection of organic ligands can control the configuration of supramolecular assemblies possessing interesting properties. One of the important properties of these materials is framework flexibility [20]. Structural transformations with the breaking, making, or rearrangement of bonds are driven by chemical and physical stimuli in which the transformations are generally accompanied by removal or exchange of solvent and/or guest, changes in coordination number of metal containing nodes, and conformation changes in flexible parts of organic ligands [21]. Nevertheless, producing molecular materials from organic ligands and metal ions to generate novel supramolecular architectures is still a challenge.

Nitrogen-containing heterocycles have been widely used as ligands as they may favour the assembly of supramolecular architectures by establishing a variety of non-covalent interactions [22–25]. For example, it was recently reported that complexes featuring bitriazole-based ligands exhibit different structures depending on the solvent and synthesis temperature [26]. In particular, mixed N, S- or N, O-heterocycles, such as thiazoles and oxazoles have

received much attention [27–30]. Recently, thiazolecarboxylic acids were chosen as potential organic ligands in crystal engineering of supramolecular structures, as the coexistence of thiazole and carboxylate moieties could afford versatile coordination ability and also establish a variety of non-covalent interactions generating infinite multidimensional supramolecular structures ranging from zero to three dimensions [31–33]. Nevertheless, studies on transition metal complexes incorporating these ligands are relatively sparse. In our previous work, we have observed the [N,O]-chelation property of thiazole-4-carboxylate ligand to some first row transition metals through its nitrogen atom and the carboxylate forming 0D molecular structures [31]. However, moving the carboxyl group from the 4- to the 5-position of the heterocyclic ring could lead to bridging rather than chelating ligand, but might alternatively form [S,O]-chelates.

Herein, we describe the nascent coordination chemistry of thiazole-5-carboxylic acid (5-Htza). The crystal structures of 5-Htza (**L**) and three new coordination polymers 1D [Cu₂(5-tza)₂(phen)₂(NO₃)₂] (**1**), 2D [Cu(5-tza)₂(MeOH)₂] (**2**), and 3D [Cu(5-tza)₂]·H₂O (**3**) coordination polymers have been obtained by X-ray diffraction. These structures, their interconversion, and thermal behaviour are described here.

2. Experimental

2.1. Materials and instruments

Chemical reagents were purchased commercially and were used as received without further purification; Cu(NO₃)₂·2.5H₂O (Alfa Aesar, 99%), thiazole-5-carboxylic acid (C₄H₃NO₂S, Apollo Scientific), 2,2'-bipyridine (C₁₀H₈N₂, Alfa Aesar, 99.0%), 1,10-phenanthroline (C₁₂H₈N₂, Sigma-Aldrich, 99.0%), methanol (VWR Chemicals, 100%).

Elemental analysis was performed on a Fisons - EA1108 CHNS/O Element Analyzer. The X-ray powder diffraction (PXRD) experiments were conducted using a PANalytical Empyrean X-ray diffractometer. IR spectra were collected in a range of 4000-600 cm^{-1} , using a Thermo Scientific Nicolet iS5 FT-IR Spectrometer. The IR spectrum of each compound is reproduced in the Supplementary Information. Thermogravimetric-differential thermal analysis (TG/DTA) was conducted using a TGA/DSC 1 thermogravimetric analyzer instrument from 30 – 900 $^{\circ}\text{C}$ with a heating rate of 20 $^{\circ}\text{C}\cdot\text{min}^{-1}$ operating under air.

2.2. Crystallization of 5-Htza (**L**)

In an attempt to synthesize a copper complex with 5-Htza and 2,2'-bipyridine, we unexpectedly obtained brown crystals of 5-Htza. In typical experiment, $\text{Cu}(\text{NO}_3)_2\cdot 2.5\text{H}_2\text{O}$ (0.0232 g, 0.100 mmol), 5-Htza (0.0129 g, 0.100 mmol) and 2,2'-bipyridine (2,2'-bipy, 0.0156 g, 0.100 mmol) were dissolved in 5.0 mL of methanol in small vial which was closed using lid with a small pin hole. The vial was left undisturbed under room temperature. After a week, a few brown blocks crystallized from the solution and was isolated for X-ray data collection. Elemental Anal. Calcd for 5-Htza (**L**) (%): C, 37.20; H, 2.34; N, 10.85; S, 24.82. Found (%): C; 37.34; H, 2.33; N, 10.69; S, 24.75. Yield based on 5-Htza: 64%. IR (cm^{-1}) for **L**: 3072s, 1687vs, 1521w, 1465w, 1314m, 1291m, 1235m, 1095m, 1000s, 897s, 859s, 785m, 750s, 655m.

2.3. Synthesis of $[\text{Cu}_2(5\text{-tza})_2(\text{phen})_2(\text{NO}_3)_2]$ (**1**)

The synthesis of **1** was carried out as described above for **L** except that 1,10-phenanthroline (phen, 0.0180 g, 0.100 mmol) was used instead of 2,2'-bipy. Elemental Anal. Calcd for $[\text{Cu}_2(5\text{-tza})_2(\text{phen})_2(\text{NO}_3)_2]$ (**1**) (%): C, 42.29; H, 2.32; N, 12.91; S, 7.39. Found (%):

C; 43.86; H, 2.28; N, 12.51; S, 7.79. Yield based on Cu: 96%. IR (cm^{-1}) for **1**: 3104m, 1607m, 1575s, 1528m, 1426m, 1392s, 1364m, 1341w, 1313s, 1222w, 1104s, 1041w, 916m, 841m, 790m, 717s, 649m.

2.4. Synthesis of $[\text{Cu}(5\text{-tza})_2(\text{MeOH})_2]$ (**2**)

The synthesis of **2** was carried out as described above for **L** without the presence of 2,2'-bipy. Elemental Anal. Calcd for $[\text{Cu}(5\text{-tza})_2(\text{MeOH})_2]$ (**2**) (%): C, 31.29; H, 3.15; N, 7.30; S, 16.71. Found (%): C; 31.35; H, 3.16; N, 7.26; S, 16.78. Yield based on Cu: 95%. IR (cm^{-1}) for **2**: 3546m, 3440m, 3116m, 1620m, 1584s, 1536m, 1431m, 1350vs, 1220m, 1095s, 913m, 841m, 772s, 693m.

2.5. Synthesis of $[\text{Cu}(5\text{-tza})_2]\cdot\text{H}_2\text{O}$ (**3**)

Layering of solutions of different reagents has been proved to be an effective way to obtain the crystals of **3** with suitable quality for single crystal X-ray diffraction experiment. 5-Htza (0.0129 g, 0.100 mmol) was dissolved in 2.5 mL of deionized water to make yellow solution **A**, using a small test tube. Solution **B** was separately prepared by dissolving $\text{Cu}(\text{NO}_3)_2\cdot 2.5\text{H}_2\text{O}$ (0.0232 g, 0.100 mmol) in 2.5 mL of methanol. The blue solution **B** was then added slowly on top of solution **A**. The two layers started to mix at the interface giving a green mixing region in which the green crystals of **3** crystallized after two days. Elemental Anal. Calcd for $[\text{Cu}(5\text{-tza})_2]\cdot\text{H}_2\text{O}$ (**3**) (%): C, 28.44; H, 2.39; N, 8.29; S, 18.98. Found (%): C; 29.16; H, 2.35; N, 8.16; S, 19.12. Yield based on Cu: 70%. IR (cm^{-1}) for **3**: 3350m, 3447m, 3116m, 1591vs, 1538s, 1399s, 1356vs, 1296w, 1221w, 1100m, 928w, 821m, 772m, 615w.

2.6. Structural transformation experiment from **2** to **2a** and **3**

Green crystals of **2** were heated to 100 °C in a vial in an oven in air. A blue-grey solid of **2a** was obtained after 2 hours of heat treatment. Then the desolvated compound **2a** was left exposed to air for 36 hours at ambient temperature after which a teal-coloured solid of **3** was obtained. Complex **2** can also directly transform to **3** upon standing in air for 24 hours without heating.

2.7. Crystal structure determination

The sets of X-ray diffraction intensity data from **L**, **1**, **2** and **3** were collected in series of ω -scans using a Stoe IPDS2 image plate diffractometer operating with Mo $K\alpha$ radiation at 150(2) K. For **1**, **2**, and **3** a multi-scan method was applied for the absorption corrections of the collected data [34]. The structures were solved using dual-space methods within SHELXT and full-matrix least squares refinement was carried out within SHELXL-2014 *via* the WinGX program interface [35,36]. All non-hydrogen positions were located in the direct and difference Fourier maps and refined using anisotropic displacement parameters. Crystal structure data for the compounds reported here are summarized in Table 1.

Figures representing portions of the crystals structures were drawn with the following programs: Diamond [37] (Figs 1a, 2, 4, 6); Mercury [38] (Fig 1b); CrystalMaker [39] (Figs 3, 5, 7, 11, 12); Ortep-3 [40] (Fig 8).

In order to study the phase transformation of **3** upon heat treatment, the same crystal of **3** used for structure determination was remounted and glued to a glass fibre. The crystal was heated on the instrument from room temperature to 383 K in a nitrogen gas cryostream and held there for 1 hour. Then it was cooled down with a cooling rate of 6 K/min to 150 K. The X-ray

diffraction intensity data set of the crystal after cooling was collected. The collected data was treated in that same way as described for **3** before heating.

3. Results and discussion

3.1. Description of crystal structures

3.1.1. Crystal structure of 5-Htza (**L**)

Thiazole-5-carboxylic acid (5-tza) crystallizes in an orthorhombic cell with space group *Pbcm*, with a single 5-tza molecule in the asymmetric unit as shown in Fig. 1a. The molecule lies on the mirror plane and so the whole molecule is strictly planar and the carboxyl group is coplanar with the thiazole ring. The OH moiety of the carboxylic group acts as hydrogen-bond donor and the nitrogen atom of the thiazole ring as hydrogen-bond acceptor. Furthermore, the carbonyl oxygen atom acts as bifurcated acceptor in which it hydrogen bonds to H3 and H4 from the neighbour aromatic rings. Details of hydrogen bonds are listed in Table 2. These hydrogen bonding interactions lead to the formation of a two dimensional arrangement of molecules in the crystal packing in the *xy* plane (Fig. 1b). Each 2D sheet is further held together by an abundant off-set π - π stacking interaction between the aromatic rings, [$d(\text{thiazole ring centroids}) = 3.687(10) \text{ \AA}$], generating an ordered assembly along the *c* axis.

3.1.2. Crystal structure of $[\text{Cu}_2(5\text{-tza})_2(\text{phen})_2(\text{NO}_3)_2]$ (**1**)

The complex $[\text{Cu}_2(5\text{-tza})_2(\text{phen})_2(\text{NO}_3)_2]$ crystallizes in monoclinic space group *C2/c*. The asymmetric unit contains two unique Cu^{2+} ions, Cu1 and Cu2, one 5-tza ligand, two halves of a phen ligand and one nitrate anion. The whole structure of **1** can be generated by a rotation around the two fold axis passing through the two Cu atoms (Wyckoff position 4e (2)) in the

asymmetric unit (Fig. 2). The Cu1 atom is hexacoordinated by two nitrogen atoms from two different, bridging, 5-tza ligands with Cu1–N1 distance of 2.023(2) Å, a pair of nitrogen atoms from chelating phen ligand with Cu1–N2 distance of 2.037(2) Å and two oxygen atoms from two monodentate nitrate anions with Cu1–O3 distance of 2.422(2) Å, and the coordination geometry can be described as distorted octahedral. The Cu2 atom has a similar coordination environment, but it is hexacoordinated to two nitrogen atoms of chelating phen ligand with Cu1–N3 bond length of 2.014(3) Å, and two pairs of chelating 5-tza ligands with Cu1–O1 and Cu1–O2 bond lengths of 1.9924(19) and 2.4868(17) Å. Compared to the equatorial bonds, the longer distances of the axial bonds are expected due to the Jahn-Teller effect of the Cu²⁺ ion. The 5-tza ligand also bridges the two independent Cu²⁺ centres in $\mu_2\text{-}\eta^2\eta^1$ manner to form a zigzag polymer chain propagating along the [001] direction (see Fig. 3). For coordinated carboxylate, the value of Δ , where $\Delta = \nu_{\text{asym}}(\text{CO}_2) - \nu_{\text{sym}}(\text{CO}_2)$, has been used to confirm and identify the mode of coordination [41]. Here, the value of Δ is 183 cm⁻¹ which is consistent with the asymmetric bidentate coordination of the carboxylate. Intermolecular O–H \cdots O and C–H \cdots O hydrogen bonding interactions (Table 2) together with π - π stacking interaction between two adjacent phen rings contribute to the consolidation of the 3D supramolecular architecture. It is notable that very similar reaction conditions employing 2,2'-bipy instead of phen do not lead to coordination by the ligand. We do not fully understand the reasons for this, but the apparent inertness must be due to the slightly more basic nature and better complexation ability of phen.

3.1.3. Crystal structure of [Cu(5-tza)₂(MeOH)₂] (2)

The compound [Cu(5-tza)₂(MeOH)₂] (2) crystallizes in the monoclinic space group $P2_1/n$ with two molecules per unit cell. The asymmetric consists of one Cu²⁺ ion, one 5-tza ligand and

a methanol molecule. Therefore, only half of the complex is present in the asymmetric unit, which is related to its other half by an inversion centre located at the Cu atom (Fig. 4). The coordination sphere of the Cu²⁺ centre takes an elongated octahedral geometry with the equatorial plane occupied by four molecules of 5-tza ligands; two are bound through the nitrogen atom with a Cu–N distance of 2.0045(18) Å and two are bound through monodentate carboxylate with a Cu–O distance of 1.9705(16) Å. Both N atoms and carboxyl O atoms are in a *trans* conformation with respect to each other. Two methanol molecules complete the coordination sphere in the axial positions with a Cu–O_{MeOH} distance of 2.459(15) Å. Thus, the 5-tza acts as a μ_2 - $\eta^1 \eta^1$ bridging ligand in which it links the adjacent metal centres through the heterocyclic N atom and the carboxyl O atom. The carboxylate is monodentate and the observed value of Δ is 234 cm⁻¹ which, as expected, is greater than for compound **1**, and consistent with other examples [41].

The resulting network is thus symmetric and planar 2D sheets are formed in the *xz* plane (Fig. 5a). Topological analysis using TOPOS software, by taking Cu²⁺ ions as nodes and 5-tza ligands as linkers, indicates that the complex of [Cu(5-tza)₂(MeOH)₂] exhibits a uninodal 4-connected non-interpenetrated **sql/Shubnikov** tetragonal plane net with a Schläfli symbol of 4⁴.6² [42] (sometimes called a square grid). It reveals that the framework structure of the complex belongs to the same topological family as that of previously reported [Cu(5-tza)₂].1.5H₂O complex [33]. The three dimensional supramolecular structure is formed by AAA stacking of the planar sheets generating rhombic channels along the *c* crystallographic axis where the coordinating methanol molecules are located in the channels (Fig 5b). For the weakly coordinating methanol molecules, the empty accessible volume generated by removal of these

solvent molecules (calculated through the Platon/Squeeze software) [43] is 211.3 Å³, corresponding to 29% of the unit cell volume.

3.1.4. Crystal structure of [Cu(5-tza)₂]-H₂O (**3**)

Complex **3** can be described as a three dimensional framework that crystallizes in the monoclinic space group $P2_1/n$ with four molecules in the unit cell. There is one Cu²⁺ ion and two 5-tza ligands and an unbound water molecule per asymmetric unit. The coordination geometry for the pentacoordinated Cu²⁺ ion is best described as a distorted square pyramid with two aromatic N atoms and two carboxyl O atoms on the basal plane and another one carboxyl O atom at the apical position (Fig. 6). The Cu–N bond lengths fall in the range of 2.0064(13) to 2.0153(13) Å whereas the Cu–O bond lengths vary from 1.9680(11) to 2.3074(13) Å. The distortion of the square pyramid can be quantitatively characterized using the parameter τ as defined by Addison *et al.* ($\tau = 1$ for a trigonal bipyramid and 0 for square pyramid) [44]. The calculated value τ of 0.34 reveals a moderate degree of distortion of the coordination polyhedron away from a square pyramid. Regarding modes of coordination of the organic ligand, two different modes including bridging $\mu_3-\eta^1\eta^1\eta^1$ and $\mu_2-\eta^1\eta^1$ modes are present. Two of five 5-tza ligands that surround the metal centre serve as a $\mu_3-\eta^1\eta^1\eta^1$ bridging species in which its carboxylate group bridges two Cu²⁺ ions leading to the formation of a dimer. The 5-tza aromatic N atom also connects this dimer to another adjacent dimer. In addition, the other three 5-tza ligands have a $\mu_2-\eta^1\eta^1$ connection mode which apparently facilitates the formation of a three-dimensional porous structure with the channels along a axis (Fig. 7a). The carboxylate here displays two different modes of coordination, both bridging and monodentate. Two values for Δ

can be obtained from the FT-IR spectrum of **3**. $\Delta = 192 \text{ cm}^{-1}$ is consistent with the bridging mode and $\Delta = 235 \text{ cm}^{-1}$ is in the range expected of a monodentate carboxylate. [41]

A better insight into the nature of this framework can be achieved by the application of a topology approach, i.e. reducing multidimensional structures to simple node and connection nets. If the dimer is taken as a node and the 5-tza as a linker, the 3D framework of **3** can be simplified as an 8-connected uninodal **bcu body centered cubic** net with Schläfli symbol $4^{24}\cdot 6^4$ [42], as shown in Fig. 7b. The unbound water molecules are located in the channels and form O–H \cdots O hydrogen bonded to the non-coordinating carboxyl O atoms of 5-tza ligands (Table 2).

An attempt to study the structural transformation of **3** upon heating has been made. A single crystal was heated for 60 minutes in a nitrogen gas cryostream to 383 K (a sensible maximum for our system). A slight clouding of the crystal faces was observed after heat treatment but the shape and colour of the crystal did not alter. The crystal was cooled to 150 K for X-ray data collection. The single crystal X-ray diffraction data reveal that the structures of the crystal before and after heating are identical. (See CCDC 1501112.) None of the unbound water molecules have been removed during the heating process, indicating the strong hydrogen bonding interactions between these water molecules and the framework. The retention of the uncoordinated water following heat treatment in a gas flow at 383 K is unexpected, but the reason for this is clear in the structure. The water molecule forms a ring of hydrogen bonds with graph set $R_4^4(8)$ that localise it within the structure (Fig. 8). Following this experiment, we collected TGA data on **3**, which is contained within the supplementary information. The decomposition of **3** starts a little above 110 °C; the broad first weight loss occurs over around 100 °C and leads to a reduction of 18.3 % mass. This is too large to be simply loss of water, so is perhaps associated with decomposition of the ligand. A second, larger, much more rapid, weight

loss begins at 211 °C and is complete by 250 °C. This corresponds to decomposition of the ligand and a further 47.3 % weight loss. There is no evidence for further, thermally stable phases that contain the thiazole ligand. There are further broad weight losses until a final mass of 20.5 % is reached upon heating to 950 °C.

3.2. Thermal properties of **2**

The thermogravimetric profile (Fig. 9) of **2** reveals the partial loss of the coordinating methanol molecules starts at about 30 °C. A complete removal of methanol molecules from crystalline material is achieved around 110 °C corresponding to the weight loss of approximately 13.3% (calc. 16.7%). The desolvated product thus can be composition $[\text{Cu}(5\text{-tza})_2]$. Apparently, the desolvated product possesses high thermal stability up to 190 °C. Above 190 °C, the weight loss of 64.7% began which corresponds to the decomposition of organic ligands (calc. 67.2%). At the end of analysis, 20.5% of ash remains.

3.3. Structural transformation induced by methanol removal of **2**

We observed an irreversible structural transformation of **2** upon removal of coordinating methanol molecules (Fig. S2). When the green crystals of **2** were exposed to air at room temperature for 24 hours, a teal-coloured crystalline material was obtained which was proved to have the same network as complex **3** through PXRD patterns as shown in Fig. 10. Although **2** and **3** have the same crystal system and space group, monoclinic $P2_1/n$, their unit cell parameters are significantly different, resulting in differences in unit cell volume (Table 1). The structural transformation from 2D sheet to 3D coordination polymer is mainly due to the breaking of the weak Cu–O_{3MeOH} bonds [$d(\text{Cu}–\text{O}_{3\text{MeOH}}) = 2.4612(15) \text{ \AA}$] in **2** and the formation of new Cu–O₅.

{tza} bonds in **3**. The loss of coordinating methanol molecules in **2** produces free coordination sites on the Cu²⁺ ion and also enabled the adjacent 2D sheets to approach each other. In the pristine solid the sheets are 6.195 Å apart and nearest copper ions are at a distance 7.467 Å. The transformation involves a translation of one layer relative to the next of around 4.2 Å to align the copper centres. This allows the neighbouring unbonded carboxyl O atom to attack on a free site of Cu²⁺ centre and thereby form Cu–O{5-tza} bond, altering the coordination geometry from original distorted octahedral to distorted square pyramidal (see Fig.11 and Fig. 12). This produces a dimer of Cu²⁺ ions bridged by two carboxylates with the metal ions 4.193 Å apart. Compared to **2**, the presence of both $\mu_3\text{-}\eta^1\eta^1\eta^1$ and $\mu_2\text{-}\eta^1\eta^1$ bridging modes of the 5-tza ligands in **3** plays a crucial role on the formation of the 3D coordination polymeric structure.

Alternatively, heating of the green crystals of **2** at 373 K for 2 hours results in a blue-grey powder of the desolvated product **2a**. This was analysed immediately by X-ray powder diffraction. According to the PXRD patterns as shown in Fig. 10, compound **2a** is very similar to the known complex [Cu(5-tza)₂] \cdot 1.5H₂O; presumably it is the empty form of [Cu(5-tza)₂] \cdot 1.5H₂O [33]. The pristine form of [Cu(5-tza)₂] \cdot 1.5H₂O [33] contains a square grid of Cu²⁺ ions linked by 5-tza bound through nitrogen and through chelating carboxylate. Between this grid are located disordered water molecules. The structural transformation of **2** to **2a** by removal of methanol by heat treatment occurs with limited structural change. The crystal of [Cu(5-tza)₂] \cdot 1.5H₂O bears a close resemblance to that of **2** as each have the same crystal system and space group, monoclinic *P2₁/n*, and similar unit cell parameters (Table 1). The transformation from **2** to **2a** involves loss of methanol, breaking of Cu–O_{3MeOH} bonds [$d(\text{Cu–O}_{3\text{MeOH}}) = 2.4612(15)$ Å], and the formation of new Cu–O_{25-tza} bonds [$d(\text{Cu–O}_{25\text{-tza}}) = 2.5993(5)$ Å] *ie* the carboxylate changes from being monodentate to bidentate. The two dimensional sheets along

[101] direction are preserved in the desolvated complex. Thus, the coordination number of Cu^{2+} centre does not change and the structure still retains the 2D layer. However, this change in ligand coordination modes; from a $\mu_2\text{-}\eta^1\eta^1$ mode in **2** to $\mu_2\text{-}\eta^2\eta^1$ mode in **2a**, affects the orientation of the planar sheets in crystal packing in which the sheets move closer to each other generating the square channels running along the crystallographic *a* axis.

When the desolvated product **2a** was placed in air, a colour change from blue-grey to teal was observed after a few hours. After 12 hours in air, the PXRD pattern (Fig. 10) was substantially different and corresponded to almost complete transformation to **3**. The small peak at 12.6° shows there is some form **2a** still present. After 36 hours, the transformation is complete. This transformation involves the cleavage of $\text{Cu-O}_{5\text{-tza}}$ [$d(\text{Cu-O}_{5\text{-tza}}) = 2.5993(5) \text{ \AA}$] bond in **2a** and the generation of new $\text{Cu-O}_{5\text{-tza}}$ bond in similar way as described for the transformation from **2** to **3** above.

3.4. Relationship to earlier work

$[\text{Cu}(5\text{-tza})_2]\cdot 1.5\text{H}_2\text{O}$ has been reported before by Rossin *et al.* [33]. They describe the desolvation of this phase (by heating to 110°C) and its subsequent ability to absorb CO_2 selectively in the presence of N_2 . However, the structural and diffraction data presented by Rossin *et al.* are ambiguous. While the PXRD pattern of the pristine solid $[\text{Cu}(5\text{-tza})_2]\cdot 1.5\text{H}_2\text{O}$ agrees with the calculated pattern for the single crystal structure (see Rossin *et al.* [33], Fig. S9), the material that has been stored at room temperature and then heated has a different pattern, although the authors do not mention this (see Rossin *et al.* [33], Fig. 5). We have examined the earlier diffraction data presented for $[\text{Cu}(5\text{-tza})_2]\cdot 1.5\text{H}_2\text{O}$ in the light of our findings and identified the phases present. This is dominated by a phase with a diffraction pattern similar to

[Cu(5-tza)₂] \cdot H₂O (**3**), of unknown hydration, and a small amount of the pristine phase [Cu(5-tza)₂] \cdot 1.5H₂O. In a similar way to our findings, Rossin *et al.* have used a sample which has transformed from a 2D to a 3D structure, perhaps with the loss of some water. This finding helps to explain the gas sorption reported previously; the selective absorption of CO₂ over N₂ is happening in a 3D framework with relatively limited channels that have a highly polar lining. The comparison of previously reported diffraction data and ours is in Fig. S1.

4. Conclusions

We succeeded in the design and syntheses of novel coordination polymers containing thiazole-5-carboxylate. The 5-tza has been found to be a good bridging ligand for the construction of Cu²⁺ coordination polymers with a variety of modes of coordination. The 5-position of the carboxyl group on the thiazole ring provides a predictable bridging mode of coordination rather than the [N,O]-chelating one observed for its analogous molecules bearing the same functional group in the 2- and 4-position. From this perspective, this study has to be considered as a step towards the synthesis of thiazole-based supramolecular networks as well as metal organic frameworks (MOFs) for use as functional materials in the future.

Acknowledgments

The work is funded by the Thailand Research Fund and the National Research University Project. N. Meundaeng thanks to the Science Achievement Scholarship of Thailand and the Graduate School, Chiang Mai University for the Ph.D. scholarships. We are grateful to Mr. Ian Dobson for assistance in collection of thermogravimetric data.

Appendix A. Supplementary information

CCDC 1500629-1500632 and 1501112 contains the supplementary crystallographic data for this paper. These data can be obtained free of charge from The Cambridge Crystallographic Data Centre via www.ccdc.cam.ac.uk/data_request/cif. Supplementary information describes relationship between our phases and previously reported work.

References

- [1] G.R. Desiraju, *Acc. Chem. Res.* 35 (2002) 565-573.
- [2] D.C. Sherrington, K.A. Taskinen, *Chem. Soc. Rev.* 30 (2001) 83-93.
- [3] A.J. Blake, N.R. Champness, P. Hubberstey, W.S. Li, M.A. Withersby, M. Schröder, *Coord. Chem. Rev.* 183 (1999) 117-138.
- [4] W. Lin, O.R. Evans, R.G. Xiong, Z. Wang, *J. Am. Chem. Soc.* 120 (1998) 13272-13273.
- [5] N. Lopez, T.E. Vos, A.M. Arif, W.W. Shum, J.C. Noveron, J.S. Miller, *Inorg. Chem.* 45 (2006) 4325-4327.
- [6] M. Shu, C. Tu, W. Xu, H. Jin, J. Sun, *Cryst. Growth Des.* 6 (2006) 1890-1896.
- [7] W. Yang, A. Greenaway, X. Lin, R. Matsuda, A.J. Blake, C. Wilson, W. Lewis, P. Hubberstey, S. Kitagawa, N.R. Champness, M. Schröder, *J. Am. Chem. Soc.* 132 (2010) 14457-14469.
- [8] H. Wang, J. Xu, D.S. Zhang, Q. Chen, R.M. Wen, Z. Chang, X.H. Bu, *Angew. Chem. Int. Ed. Engl.* 54 (2015) 5966-5970.
- [9] M.J. Zaworotko, *Chem. Commun.* 1 (2001) 1-9.

- [10] Y.Y. Liu, Y.Q. Huang, W. Shi, P. Cheng, D.Z. Liao, S.-P. Yan, *Cryst. Growth Des.* 7 (2007) 1483-1489.
- [11] B.C. Tzeng, Y.C. Hung, G.H. Lee, *Chem. Eur. J.* 22 (2016) 1522-1530.
- [12] H.Y. Deng, J.R. He, M. Pan, L. Li, C.Y. Su, *Cryst. Eng. Comm.* 11 (2009) 909-917.
- [13] P. Bhowmik, L.K. Das, A. Bauzá, S. Chattopadhyay, A. Frontera, A. Ghosh, *Inorg. Chim. Acta* 448 (2016) 26-33.
- [14] Y. Fu, Z. Xu, J. Ren, J. Yang, *Cryst. Growth Des.* 7 (2007) 1198-1204.
- [15] Y. Wei, H. Hou, Y. Fan, Y. Zhu, *Eur. J. Inorg. Chem.* 19 (2004) 3946-3957.
- [16] P. Cui, J. Wu, X. Zhao, D. Sun, L. Zhang, J. Guo, D. Sun, *Cryst. Growth Des.* 11 (2011) 5182-5187.
- [17] D. Sun, Y. Ke, T.M. Mattox, B.A. Ooro, H.C. Zhou, *Chem. Commun.* 43 (2005) 5447-5449.
- [18] H. Wang, S.J. Liu, D. Tian, J.M. Jia, T.L. Hu, *Cryst. Growth Des.* 12 (2012) 3263-3270.
- [19] L.Y. Du, W.J. Shi, L. Hou, Y.Y. Wang, Q.Z. Shi, Z. Zhu, *Inorg. Chem.* 52 (2013) 14018-14027.
- [20] Z. Chang, D.H. Yang, J. Xu, T.L. Hu, X.H. Bu, *Adv. Mater.* 27 (2015) 5432-5441.
- [21] J. Pirochom, N. Wannarit, J. Boonmak, K. Chainok, C. Pakawatchai, S. Youngme, *Inorg. Chem. Commun.* 44 (2014) 111-113.
- [22] S. Jin, H. Liu, G. Chen, Z. An, Y. Lou, K. Huang, D. Wang, *Polyhedron* 95 (2015) 91-107.
- [23] E. Sayın, G.S. Kürkçüoğlu, O.Z. Yeşilel, T. Hökelek, *J. Mol. Struct.* 1096 (2015) 84-93.
- [24] H. Li, *Synth. React. Inorg. Met.-Org. Chem.* 45 (2015) 1664-1667.
- [25] S. Yan, X. Zheng, *J. Mol. Struct.* 964 (2010) 52-57.

- [26] L.Y. Du, H. Wang, G. Liu, D. Xie, F.S. Guo, L. Hou, Y.Y. Wang, *Dalton Trans.* 44 (2015) 1110-1119.
- [27] B. Di Credico, G. Reginato, L. Gonsalvi, M. Peruzzini, A. Rossin, *Tetrahedron* 67 (2011) 267-274.
- [28] Y. Deng, H. Liu, B. Yu, M. Yao, *Molecules* 15 (2010) 3478.
- [29] A. Rossin, G. Giambastiani, *Cryst. Eng. Comm.* 17 (2015) 218-228.
- [30] L.M.T. Frija, A.J.L. Pombeiro, M.N. Kopylovich, *Coord. Chem. Rev.* 308 (2016) 32-55.
- [31] N. Meundaeng, A. Rujiwatra, T.J. Prior, *Transit. Met. Chem.* 4 (2016) 783-793.
- [32] A. Rossin, B. Di Credico, G. Giambastiani, L. Gonsalvi, M. Peruzzini, G. Reginato, *Eur. J. Inorg. Chem.* 4 (2011) 539-548.
- [33] A. Rossin, G. Tuci, G. Giambastiani, M. Peruzzini, *ChemPlusChem* 79 (2014) 406-412.
- [34] R. Blessing, *Acta Cryst.* A51 (1995) 33-38.
- [35] G.M. Sheldrick, *Acta Cryst.* A71 (2015) 3-8.
- [36] G.M. Sheldrick, *Acta Cryst.* C71 (2015) 3-8.
- [37] K. Brandenburg, M. Berndt, DIAMOND, Crystal Impact GbR, Bonn, Germany, 1999.
- [38] C.F. Macrae, P.R. Edgington, P. McCabe, E. Pidcock, G.P. Shields, R. Taylor, M. Towler, J. van de Streek, *J. Appl. Cryst.* 39 (2006) 453-457.
- [39] D.C. Palmer, CrystalMaker, CrystalMaker Software Ltd, Begbroke, Oxfordshire, England, 2014.
- [40] L.J. Farrugia, *J. Appl. Cryst.* 45 (2012) 849-854.
- [41] G.B. Deacon, R.J. Phillips, *Coord. Chem. Rev.* 33 (1980) 227-250.
- [42] V.A. Blatov, A.P. Shevchenko, D.M. Proserpio, *Cryst. Growth Des.* 14 (2014) 3576-3586.
- [43] A. Spek, *Acta Cryst.* D65 (2009) 148-155.

[44] A.W. Addison, T.N. Rao, J. Reedijk, J. van Rijn, G.C. Verschoor, *J. Chem. Soc., Dalton Trans.* 7 (1984) 1349-1356.

Table 1 Crystallographic data of **L**, **1**, **2** and **3**

| | 5-Htza (L) | [Cu ₂ (5-tza) ₂ (phen) ₂ (NO ₃) ₂] (1) | [Cu(5-tza) ₂ (MeOH) ₂] (2) | [Cu(5-tza) ₂]-H ₂ O (3) | [Cu(5-tza) ₂]-1.5H ₂ O (2a) ^a [33] |
|--|---------------------|---|---|--|--|
| Formula weight | 129.13 | 867.76 | 383.88 | 337.81 | 693.63 |
| Colour | Brown | Green | Green | Blue-green | Dark green |
| Crystal system | Orthorhombic | Monoclinic | Monoclinic | Monoclinic | Monoclinic |
| Space group | <i>Pbcm</i> | <i>C2/c</i> | <i>P2₁/n</i> | <i>P2₁/n</i> | <i>P2₁/n</i> |
| Temperature (K) | 150(2) | 150(2) | 150(2) | 150(2) | 150(2) |
| Wavelength (Å) | 0.71073 | 0.71073 | 0.71073 | 0.71073 | 0.71073 |
| <i>a</i> (Å) | 6.780(2) | 12.1710(11) | 7.4646(9) | 8.7377(7) | 6.916(5) |
| <i>b</i> (Å) | 12.082(5) | 23.2520(19) | 11.4558(11) | 10.5776(12) | 10.037(6) |
| <i>c</i> (Å) | 6.403(3) | 12.7039(11) | 8.6518(10) | 12.8766(10) | 9.874(8) |
| β (°) | 90 | 116.025(6) | 100.227(9) | 109.733(6) | 97.755(7) |
| <i>V</i> (Å ³) | 524.5(4) | 3230.7(5) | 728.09(14) | 1120.22(18) | 679.1(8) |
| <i>Z</i> | 4 | 4 | 2 | 4 | 1 |
| <i>D</i> _{calc} (g cm ⁻³) | 1.635 | 1.784 | 1.751 | 2.003 | |
| Absorption coefficient (mm ⁻¹) | | | | | |
| ¹) | 0.507 | 1.521 | 1.813 | 2.336 | |
| θ Range for data collection | | | | | |
| (°) | 1.50-29.25 | 2.15-21.35 | 3.00-29.55 | 1.70-29.45 | |
| <i>F</i> (000) | 264 | 1752 | 390 | 676 | |
| Data/restraints/parameters | 770/0/52 | 3694/0/246 | 1944/0/102 | 2995/7/175 | |
| Goodness-of-fit on <i>F</i> ² | 0.956 | 0.753 | 0.803 | 0.936 | |
| | 0.0545, | | | | |
| <i>RI</i> , <i>wR2</i> [<i>I</i> > 2 σ (<i>I</i>)] | 0.1371 | 0.0310, 0.0545 | 0.0303, 0.0568 | 0.0211, 0.0487 | |

^a [Cu(5-tza)₂]-1.5H₂O unit cell was determined from powder data and agrees with that in reference [33]

Table 2 Lists of hydrogen bonding interactions in the complexes

| D–H···A | H···A (Å) | D···A (Å) | ∠D–H···A (°) |
|-----------------------------|------------------|------------------|---------------------|
| L | | | |
| C4–H4···O1 ⁱ | 2.21 | 3.154(4) | 175 |
| C3–H3···O1 ⁱⁱ | 2.58 | 3.201(4) | 123 |
| O2–H2···N1 ⁱⁱⁱ | 1.88 | 2.669(3) | 168 |
| 1 | | | |
| C3–H3···O3 ^{iv} | 2.53 | 3.118(4) | 120 |
| C3–H3···O5 ^{iv} | 2.63 | 3.214(4) | 120 |
| C6–H6···O2 ^v | 2.51 | 3.080(4) | 118 |
| C5–H5···N1 | 2.61 | 3.115(4) | 113 |
| C5–H5···O2 ^v | 2.53 | 3.091(3) | 117 |
| C12–H12···O4 ^{vi} | 2.32 | 2.976(4) | 126 |
| C11–H11···O4 ^{vi} | 2.53 | 3.078(4) | 117 |
| C4–H4···O3 | 2.30 | 2.947(3) | 124 |
| 2 | | | |
| O3–H3A···O2 | 1.86 | 2.684(3) | 168 |
| 3 | | | |
| C4–H4···O2 ^{vii} | 2.56 | 3.055(3) | 115 |
| C4–H4···O1w ^{viii} | 2.59 | 3.113(4) | 117 |
| C8–H8···O1 ^{ix} | 2.40 | 2.885(3) | 112 |
| O1w–H1A···O4 | 1.91(2) | 2.790(3) | 167(4) |
| O1w–H1B···O4 ^x | 2.04(2) | 2.941(3) | 168(4) |

Symmetry codes: (i) $-x+2, y-1/2, -z+1/2$; (ii) $-x+1, y-1/2, -z+1/2$; (iii) $-x+1, y+1/2, -z+1/2$; (iv) $-x+1, y, -z+1/2$; (v) $-x+1/2, -y+3/2, -z+1$; (vi) $x+1/2, -y+3/2, z+1/2$; (vii) $x+1/2, -y+1/2, z+1/2$; (viii) $x+3/2, y-1/2, -z+3/2$; (ix) $-x+1/2, y+1/2, -z+1/2$; (x) $-x+1, -y+2, -z+1$.

Supplementary information to accompany ‘Copper coordination polymers constructed from thiazole-5-carboxylic acid: synthesis, crystal structures, and structural transformation’

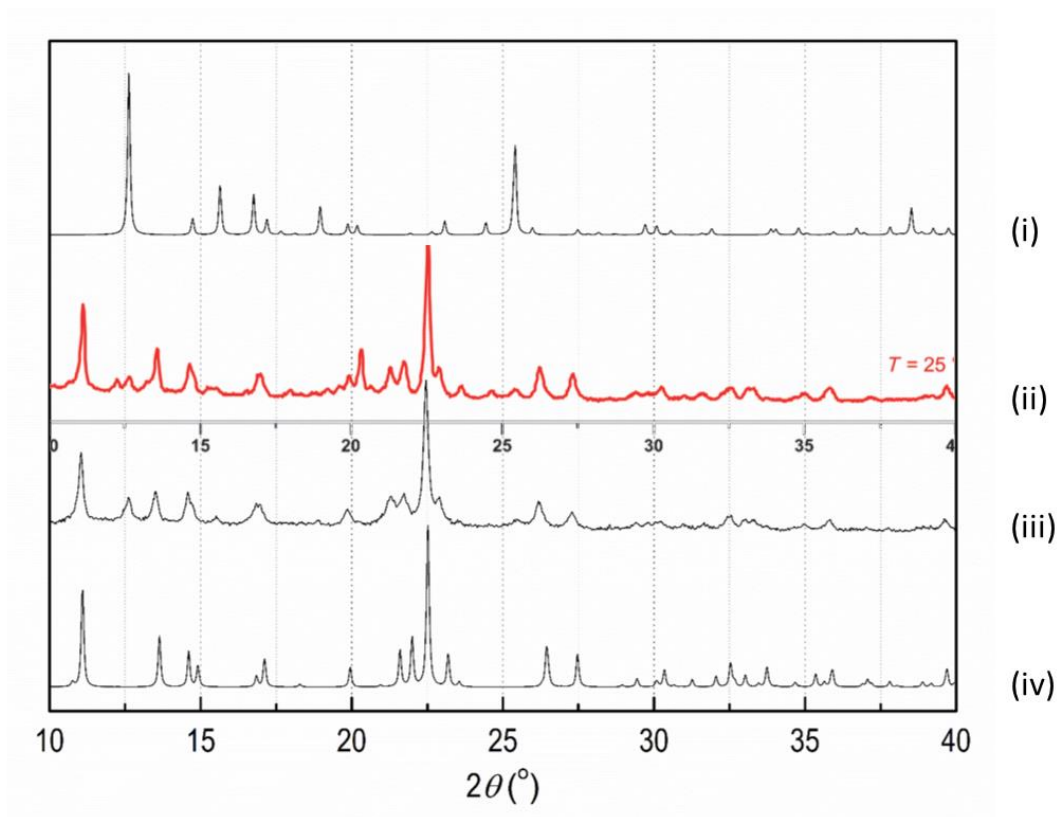


Fig. S1 PXRD patterns showing the phase transformation of **2a** to **3**:

- (i) Simulated pattern of pristine $[\text{Cu}(5\text{-tza})_2] \cdot 1.5\text{H}_2\text{O}$ (CCDC 964607)
- (ii) Pattern reported by Rossin *et al.* to be dehydrated form of $[\text{Cu}(5\text{-tza})_2] \cdot 1.5\text{H}_2\text{O}$
- (iii) (this work) pattern of **2a** left in air for 12 hours
- (iv) Simulated pattern of **3**

The pattern of the dehydrated form of $[\text{Cu}(5\text{-tza})_2] \cdot 1.5\text{H}_2\text{O}$ does not match the pattern of the pristine form well and there has clearly been a structural change. The similarity in powder diffraction patterns between (ii) and (iii) is clear and the assignment of (ii) & (iii) as dominated by a phase resembling **3**

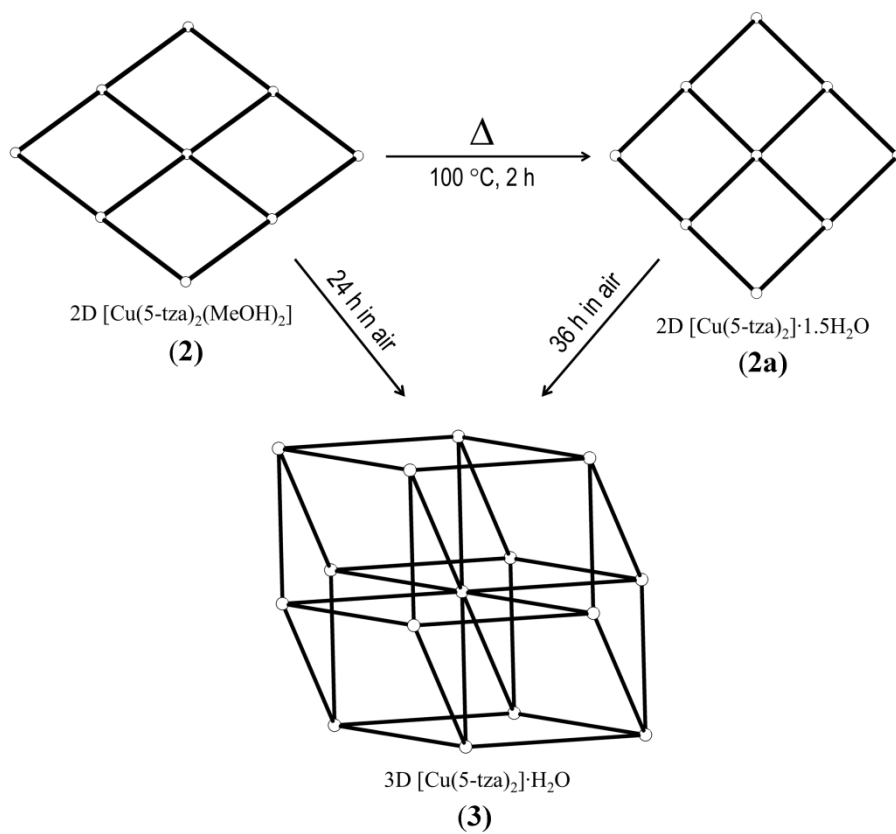


Fig. S2 Diagram showing the structural transformation of **2** to **2a** and **3** with conditions used in the experiments.

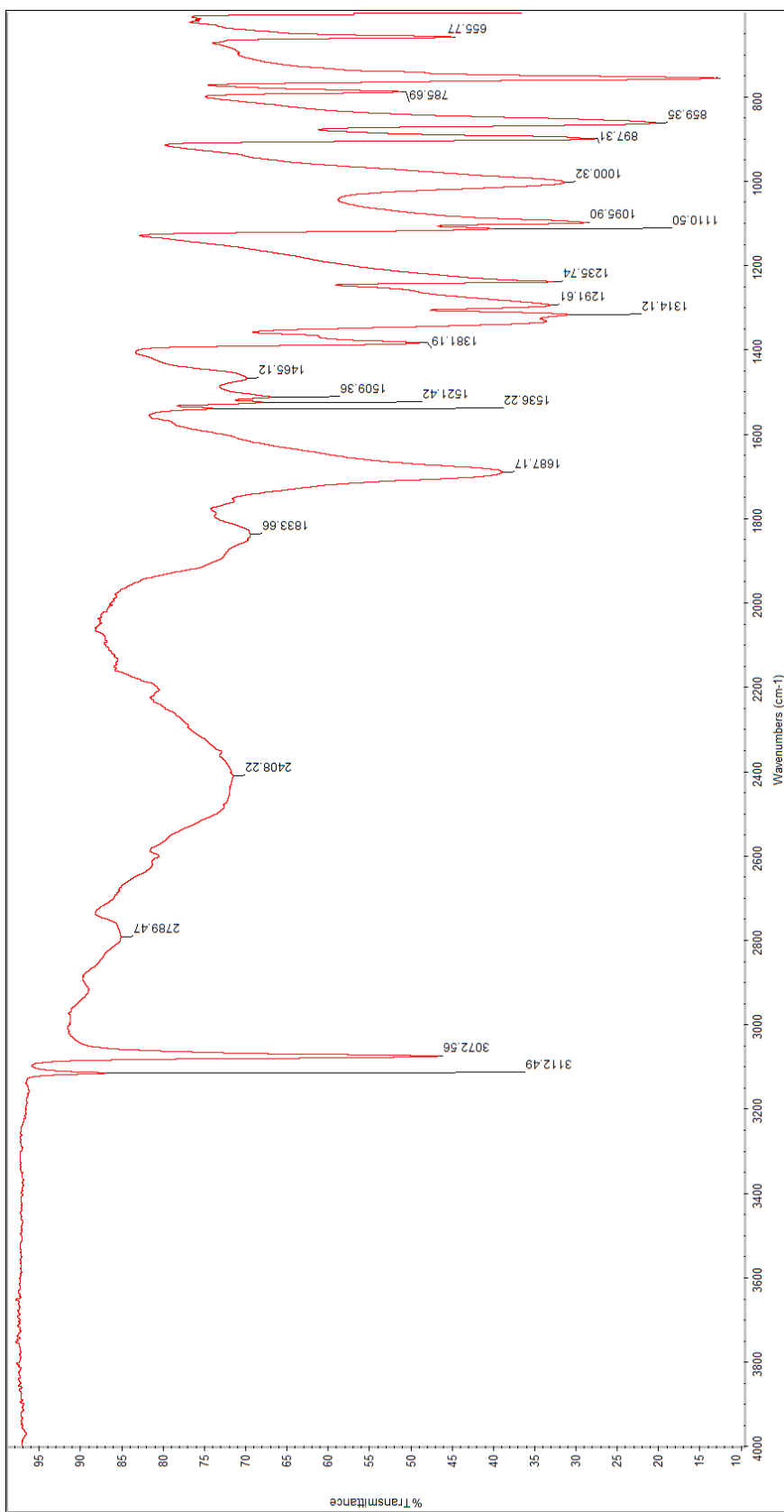


Fig. S3 IR spectrum of ligand (L)

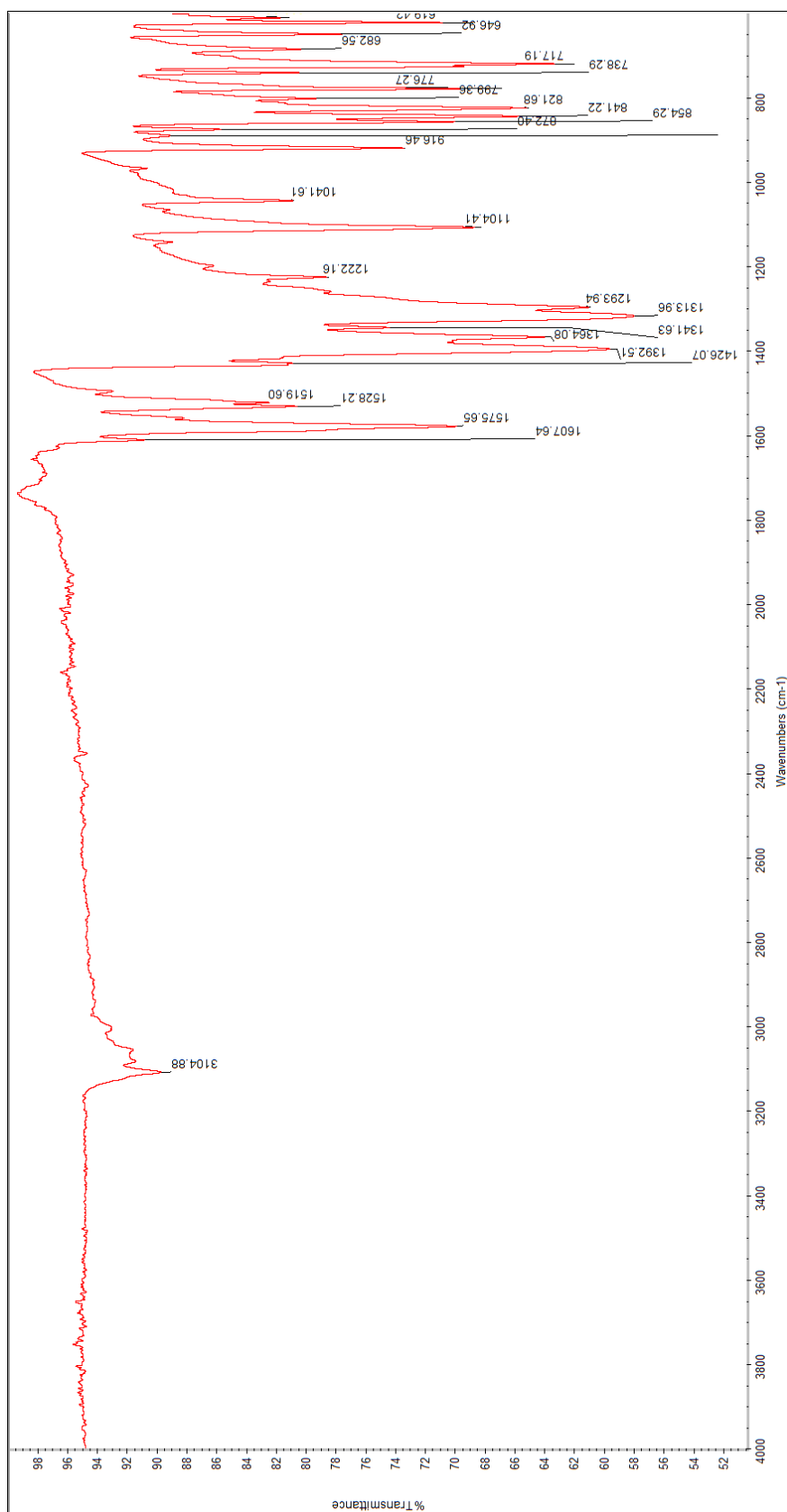


Fig. S4 IR spectrum of **1**

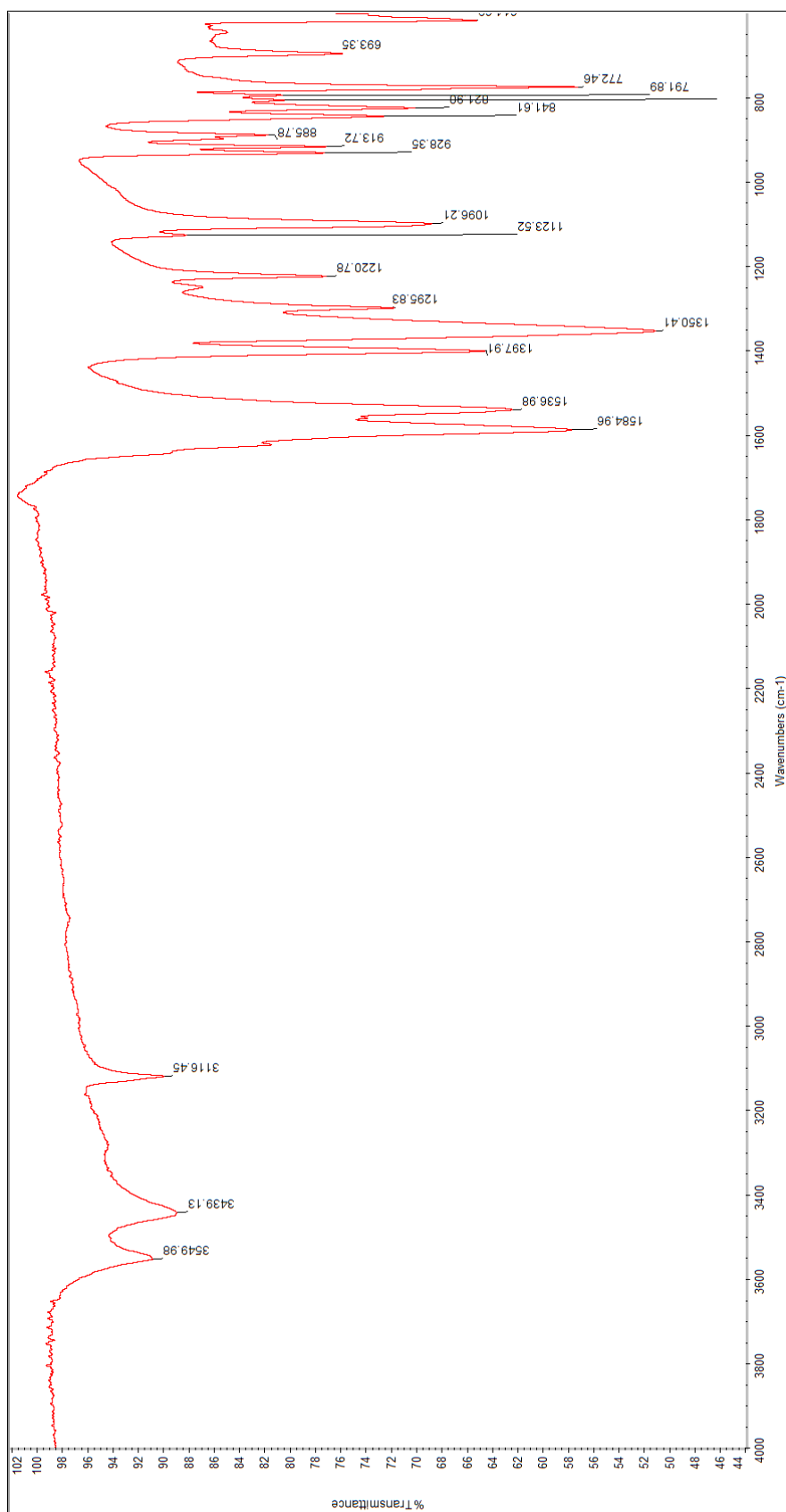


Fig. S5 IR spectrum of 2

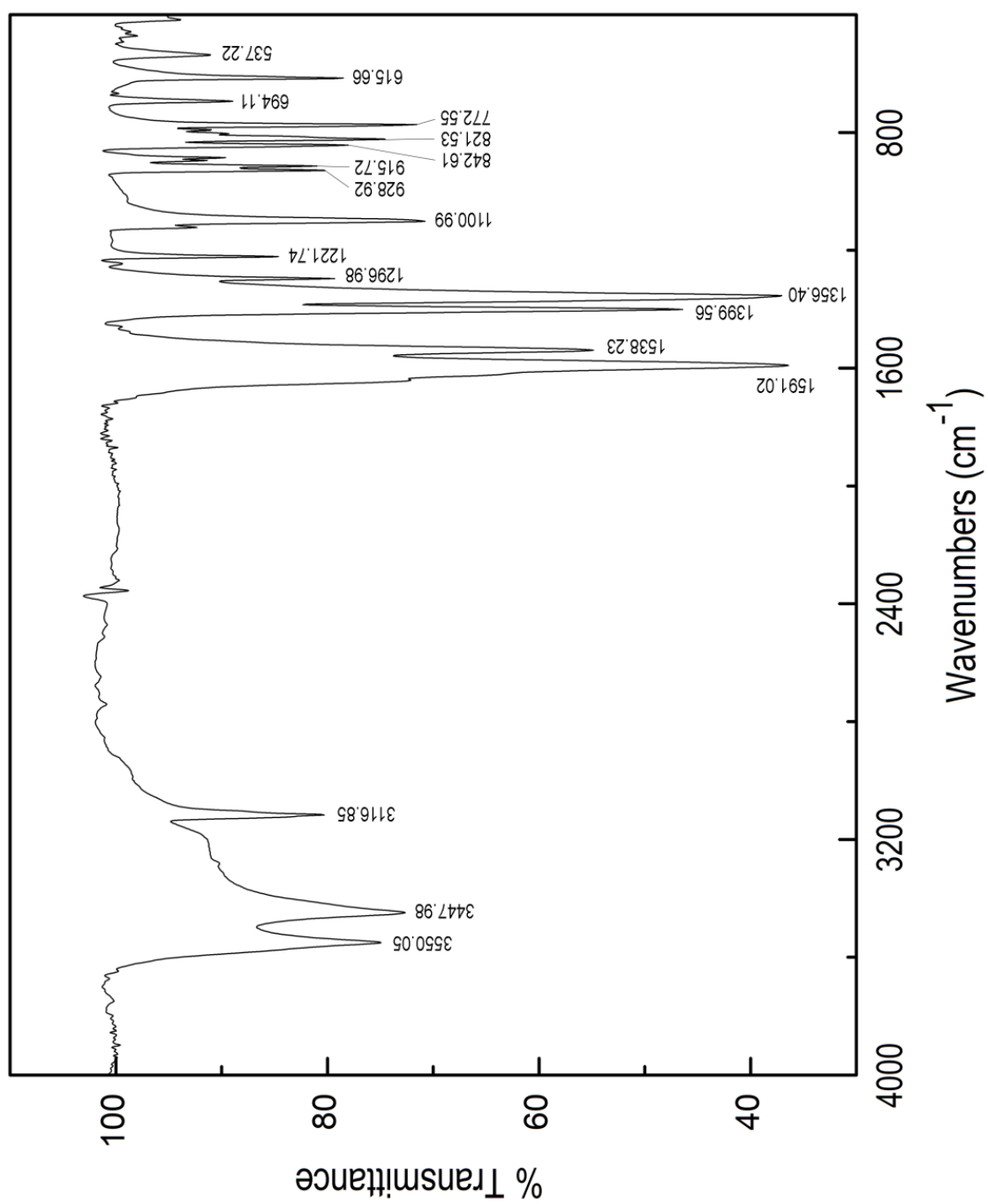


Fig. S6 IR spectrum of 3

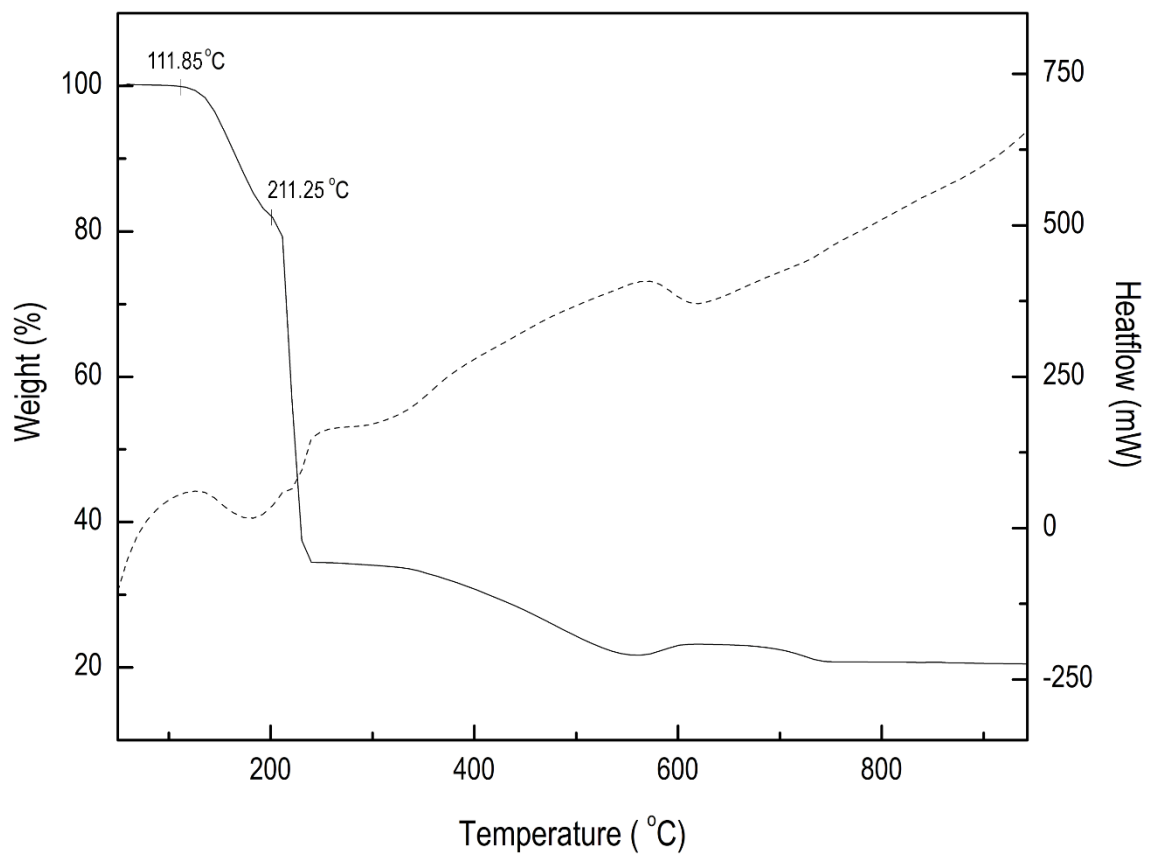


Fig. S7 The thermogravimetric profile of **3** recorded in air.